MATHEMATICAL SIMULATION OF A GLASS FURNACE

N.D. Fowkes*, C.P. Please†,
A. Hutchinson‡ and G. Fareo§

Other Study Group Participants:
S. Roy, M. Khalique, K. Jacobs, N. Mindu, A. Earle, D. Raphulu, R. Kgatle, A.H. Carrim and A. Magan

Industry Representative
Eddie Ferreira

Abstract

Both radiative heating from flames and convective heat transfer by the combustion gases significantly effect the melting rate of the batch of raw materials introduced into the oil or gas fired glass furnace. Radiative exchanges within the melting batch greatly enhance the heat transfer within the melting zone and simple Rosseland and other approximations (based on the strongly contrasting conductivities of the batch before and after melting) are used to obtain an accurate explicit analytic expression for the front speed as a function of the effective radiative

*Mathematics Department, University of Western Australia, Crawley, WA 6009, Australia *email: neville.fowkes@uwa.edu.au*

†Oxford Centre for Collaborative Applied Mathematics, University of Oxford, Oxford OX1 3LB, United Kingdom. *email: please@maths.ox.ac.uk*

‡School of Computational and Applied Mathematics, University of the Witwatersrand, Private Bag 3, WITS 2050, Johannesburg, South Africa. *email: hutchinson.ash@gmail.com*

§School of Computational and Applied Mathematics, University of the Witwatersrand, Private Bag 3, WITS 2050, Johannesburg, South Africa. *email: gidean.fareo@wits.ac.za*

input from the flame and the temperature of the combustion gases in contact with the surface of the batch. Also explicit results for the approximate temperature profile through the batch are obtained. These results are in accord with numerical simulations in the literature but are analytic and simple and thus may be more easily used for furnace design. Some preliminary observations concerning the removal of bubbles from the melted batch are made.

1 Introduction

PFG is a South African glass making company that supplies high quality plate glass for the local building industry and glass products for automobile industries. The company also exports products internationally. To avoid catastrophic glass solidification, the furnace and Pilkington float processes that produce plate glass need to operate nonstop over the lifetime of the factory, a period of fifteen years, so continuous and careful control is essential. The overriding objective is to control the quality of the final product although other efficiency and environmental issues are also important. Controlling, and perhaps improving, the operation of the furnace and its product requires a better understanding of the complex chemical and physical processes occurring within the furnace and beyond. PFG asked the MISG to examine the relevant processes. In the present article we mainly confine our attention to the furnace operation.

Flaws (usually bubbles) are 'always' present in plate glass and if the bubbles are sufficiently large they can effect the optical properties of the glass. Sheets containing unacceptable flaws are recycled, an expensive process. These bubbles have their origin in the furnace so that understanding their formation, movement and growth within the furnace and beyond is important. We will briefly describe such bubble creation and removal issues but our primary concern here will be with batch melting.

The main component of the glasses of interest is silica SiO_2, which under natural conditions occurs in a crystalline form commonly referred to as sand. The silica structure consists of SiO_4 tetrahedra joined together by means of —Si—O—Si— bridges. The oxygen atoms are shared between adjoining tetrahedra, these being strong valency bonds. When a fluxing (i.e. network modifier) material such as Na_2O is added to the crystalline material it breaks up the —Si—O—Si— bridges leading to a weaker residual valence type of inter-

action between the two silicon atoms. Thus the network is modified resulting in the amorphous transparent substance we recognise as glass. The reaction is endothermic and can only occur at high temperatures, so a furnace is required.

1.1 Furnace operation

A batch, typically consisting of ground up silica (70%), soda ash (14%) and limestone (10%) of depth 2 to 4 cms, is fed at a speed of about 1m/sec into the furnace of typical length 40m, width 10m and depth 4m containing about 1000 tons of molten glass. Being less dense the batch floats on top of already molten glass (depth about 2m) within the furnace, see Figure 1. The batch feeding process is not uniform in that it is facilitated by a barrier that moves forwards (carrying the batch into the furnace) and upwards and backwards to access the batch before moving forwards again; the input batch thus enters as mounds of material. After entry the floating layer typically splits into two separate mounds attached to the side walls of the furnace. Radiation from flames (oil or gas firing is used) melts the batch producing liquid glass which then feeds into the previously melted bath of molten glass. The floating layers of the input batch extend approximately 19m into the furnace before completely melting. Typical temperatures in the molten glass bath are 1500°C and the residence time of particles within the bath is about 10 to 15 hours. The excess glass in the furnace overflows into a second chamber through a neck at the top of the chamber, and in this second chamber temperature levels are reduced to levels (about 1400°C) appropriate for the next stage of the processing which uses the Pilkington process now described. The glass leaving the furnace is fed onto a tin tray of depth about 0.5m (width 7m) containing molten tin of depth a few cms. The liquid glass entering the tray spreads out over the melted tin forming a sheet of uniform thickness (typically 7 to 10 mm). This molten glass sheet gradually solidifies as it travels down the length of the tin bath (typically 30m) and a solid glass sheets rolls out from the end of the chamber and is cut into appropriate lengths and removed from the moving production line. As indicated earlier the whole process is continuous. For more details of the furnace see Auchet et al (2008) or Tooley (1961). An excellent mathematical analysis of the Pilkington process can be found in Howell (1994).

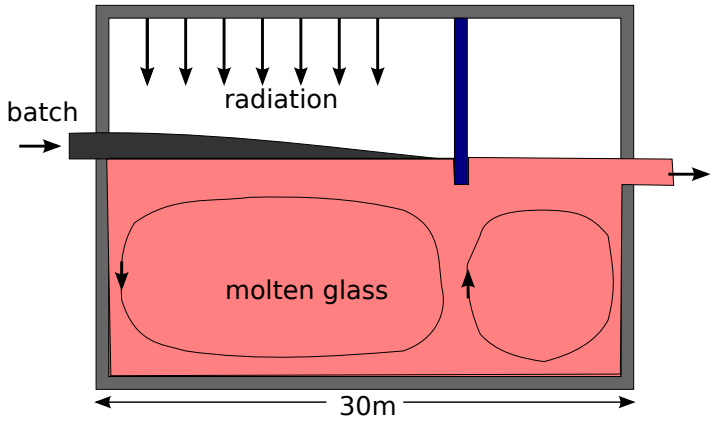

Figure 1: A glass furnace. Radiative heating from ceiling flames together with direct heating from combustion gases melt the floating batch.

1.2 The chemistry

The sodium carbonate, silicon dioxide reaction

$$n\mathrm{S}_i\mathrm{O}_2 + \mathrm{Na}_2\mathrm{CO}_3 \Leftrightarrow \mathrm{Na}_2\mathrm{O} - \mathrm{nSiO}_2 + \mathrm{CO}_2 \Uparrow \Delta\mathrm{H}_{\mathrm{chem}}, \tag{1}$$

(with n=3) typically occurs if the reaction follows the 'silica route', although other routes are possible, see Kuhn (2002). An energy input $\Delta\mathrm{H}_{\mathrm{chem}}$ (corresponding to 550 KJ/kg) is required to induce this reaction. The actual 'melting' process involves dehydration, chemical dissociation and decomposition, as well as phase transformations (crystalline solid to glassy liquid and gas), so it is preferable to formulate a global batch reaction model:

$$(1+\alpha) \text{ kg glass batch} \rightarrow 1+\alpha \text{ kg gas} + \text{energy per 1 kg glass melt},$$

which takes into account the variety of processes involved, together with their energy requirements. The energy requirements are typically 7 GJ/ton and daily production levels of 100's of tons of plate glass are typical.

Air bubbles (nitrogen and oxygen) are carried into the chamber with the batch and additionally various gases are produced both during batch melting (for example CO_2 and SiO_2 in (1)) and within the melt. Also fining agents are added to the batch to increase gas production, see later. Some of the

gas produced is immediately expelled from the batch which starts to fizz and the remainder is carried into the molten glass bath and bubbles are formed. Carbon dioxide and nitrogen are relatively insoluble in liquid glass and so form bubbles whereas the silicon dioxide produced is soluble and thus mainly remains in the melt. The bubbles may either rise to the surface forming a foam or remain within the moving melt eventually being carried out of the chamber into the next chamber, and some will be carried into the tin float chamber and will end up frozen in the glass sheet. Such bubbles are always present in the final glass sheet but only become problematic if they are large enough to significantly effect light transmission. In order to shield the second chamber from the foam a barrier (inserted from the roof) is introduced. The barrier is water cooled; lower temperature levels are required for the tin float process and also for bubble collapse, see later. Additionally bubbles are introduced into the furnace below the barrier to both sweep up small bubbles within the bath and also to increase the average glass particle residence time, thus further enabling gas bubbles to escape. Fining agents introduced into the batch also produce (large) bubbles which serve to sweep up small bubbles.

Our primary aim in Section 2 is to determine how the length of the unmelted batch within the furnace is determined by the furnace parameters. The batch blanket shape and length greatly influence heat transfer processes within the furnace and thus the fining and refining processes occurring within the melt. In Section 3 we will briefly discuss the issues associated with bubble formation and movement; there was insufficient time to undertake a serious study. Finally in Section 4 we draw conclusions and make recommendations.

2 The batch melt problem

Figure 1 diagrammatically represents the batch melting process. A batch of thickness h moving with velocity U is fed into the furnace and floats on top of previously melted glass within the furnace. Radiation from the flames (at an effective temperature of T_R) increases the temperature of the batch and melting will commence at the surface when its temperature reaches the melting point of the batch T_m. A melting front described by $z = s(t)$ will then travel down through the batch. The temperature of the melted flowing glass under the batch T_b exceeds the melting temperature of T_m of the batch mixture so that there will be also a melting front travelling upwards through the batch. The batch is totally consumed after the two fronts meet. Depending on surface

morphology and surface tension characteristics of the freshly formed melted glass this recently formed molten glass will either remain on the surface or may drain over or through the batch.

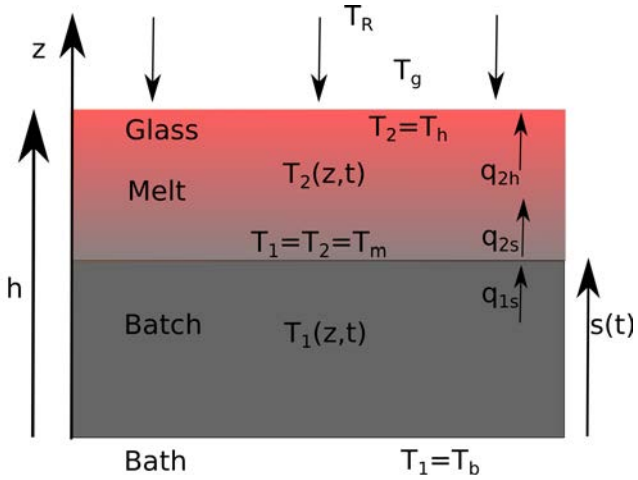

Figure 2: The melting of an element of the batch: Initially the batch occupies the region $0 < z < h$. Later the batch starts melting and we identify various regions. In the 'batch region' 1, $z < s(t)$, the batch is still intact. Melting commences if the temperature of the batch exceeds the melting temperature T_m; this occurs at $z = s(t)$. In the melt region 2, $h > z > s(t)$, melting is either complete or underway; this zone contains both solid and melted particles. The flame radiates at an effective temperature of T_R and the upper surface of the batch is bathed in gas at temperature T_g. The lower surface of the batch is in contact with already completely melted glass within the 'bath' at temperature $T_b > T_m$. The heat flux into the front from the batch is $q_{1s} < 0$, and from the front into the melt is $q_{2s} < 0$. The heat flux from the upper surface $z = h$ is q_{2h}.

Calculations suggest and we will assume that the melted glass within the batch matrix will remain in place so that a batch element will remain effectively intact until the element is completely melted.

The process is essentially a steady state process, so we can equivalently follow an element of the pile as it moves along the surface and melts, see Figure 2; the replacement $t = x/U$ can be used to recover the steady state solution.

2.1 Radiation and melting complications

A portion (about 80%) of the emitted radiation at an effective temperature T_R intercepts the batch and is absorbed; the rest is reflected or lost to the environment. At a particular location z within the melting batch this incoming radiation will intercept intact sand particles which will partially reflect and absorb the incoming radiation; no radiation is transmitted through the sand surfaces. The absorbed radiation will cause melting. The already melted glassy component of the batch at z will be (semi)transparent to incoming radiation and so the incident radiation will pass through this layer to be absorbed and reflected at lower levels. Secondary reflections from lower levels will intercept sand particles and tertiary reflections and absorptions and associated meltings will result. Additionally the sand particles and the heated glass will re-radiate in all directions and conduction will transfer heat between layers. Bubbles produced within the melting batch will also act as scatterers of radiation especially within the glassy upper layers. The net effect of the multiple internal reflections, absorptions, meltings will be to redistribute heat within the melt. There will be a layer of pure glass (completely converted batch) at the top with fractional conversion occurring down to the melting front at $s(t)$. The field equations (the semi transparent batch model) for the temperatures in the two regions $(T_1(z,t), T_2(z,t))$ are presented in Wu and Viskanta (1986) and are given by

$$\rho_1 c_1 \frac{\partial T_1}{\partial t} = \frac{\partial}{\partial z}\left(k_1(T)\frac{\partial T_1}{\partial z}\right), \qquad z < s(t),$$

$$\rho_2 c_2 \left[\frac{\partial T_2}{\partial t} + (1 - \frac{\rho_1}{\rho_2})\frac{ds}{dt}\frac{\partial T_2}{\partial z}\right] = \frac{\partial}{\partial z}\left(k_2(T)\frac{\partial T_2}{\partial z}\right) - \frac{\partial F}{\partial z} + H_2, \ z > s(t),$$

where $F(z,t)$ is the total radiative flux, and $H_2(z,t)$ is the (local) enthalpy change due to melting; we have a distributed heat sink. The bracketed term $\{\cdot\}$ on the left hand side of the second equation takes into account the volumetric change associated with the moving melting front. Boundary conditions need to be applied at the bottom and top of the batch $z = 0, h$ and Stefan conditions need to be applied at the moving front $s(t)$, see later.

The densities, specific heats and conductivities within the batch regions are (ρ_i, c_i, k_i). The specific heats c_i are temperature invariant within the zones but

different in the two zones, and the density within the melt varies depending on the degree of conversion. This density change accompaning melting will affect the location of the upper surface of the melt relative to a fixed frame but will not determine the front speed and so will be ignored here; the determination of this upper surface is of no direct importance. More significantly the conductivities vary strongly with temperature in both zones. The conductivity of sand increases exponentially by a factor of about 2 over the (room to melting temperature) range of interest, see Figure 3 and is conveniently represented in the form

$$k_1(T) = k_1^0 \exp(\gamma(T/T_0 - 1)); \tag{2}$$

where $k_1^0 = 0.3116$ is the conductivity at the input (room) temperature T_0, taken as $T_0 = 300$K, and $\gamma = 0.275$ is the exponential growth factor, see Shibata et al (2005), Wu and Viskanta (1986).

The normal thermal conductivity of melted glass is about $k_2 = 0.7$ W/(m K) and doesn't vary much with temperature, however the radiative heat exchange effects that occur in our situation require special attention.

The devil truly is in the detail here. The radiative term involves incident, emission and absorption integrals with respect to wavelength and over the partially converted melt depth, and both the radiative and enthalpy terms depend on the fraction of the melt f_b that is unconverted at (z, t). It is possible to avoid the detailed determination of $f_b(z, t)$ by making the assumption that one can identify a temperature range ΔT_m over which melting occurs and associate a 'fractional' melting temperature T_f with each f_b; explicitly

$$f_b = f_{b0} + (1 - f_{b0})(T_f - T_m)/\Delta T_m,$$

with ΔT_m about 250K. Even with this simplification the analysis is daunting.

Necessarily numerics are required to determine the solution to the above system, see Wu and Viskanta (1986) and it is not easy to usefully interpret the results obtained. Furthermore the uncertainty associated with radiation parameters suggests that detailed results are perhaps inappropriate. With this in mind we will greatly simplify the system, whilst preserving the important features.

2.1.1 Rosseland approximations

It should be noted that the effect of multiple reflections and absorptions in the reacting batch layer is to greatly increase the heat transfer through this

layer (by an order of magnitude), so the radiation 'details' needs to be addressed. Because of the complexity of radiation simulations Rosseland type approximations are often used to simplify the analysis. It can be shown, see Rosseland (1936) and Siegel and Howell (2001), that in zones that are optically thick[1] (in our case within the melt) that the net effect of multiple reflections is to increase the (molecular) thermal conductivity from k_2 by a temperature dependent (radiation) term to give an effective conductivity given by

$$k_{2\text{eff}} = k_2 + k_{2\text{radn}} \gg k_2, \quad \text{where} \quad k_{2\text{radn}} = \frac{16n^2}{3}\frac{\gamma T^3}{a_R};$$

here n is the refractive index, and a_R is an absorption coefficient calculated from the spectral absorption of the glass melt and σ is the Stefan-Boltzman constant, see Rosseland (1936) and Siegel and Howell (2001).

Using numerical semi-transparent model simulations (for $h = 2$cm) Wu and Viskanta (1986) fitted a Rosseland type diffusion description to simulations to obtain the result

$$k_{2\text{eff}} = 5.39 - 0.0217 \times T + 0.0000206 \times T^2 (\text{W/m K}), \tag{3}$$

which we write in the form

$$k_{2\text{eff}} = k_{2m}\left[(1 - \alpha(T - T_m) + \beta(T - T_m)^2\right], \tag{4}$$

where $k_{2m} \approx 7$ is identified as the conductivity of the just melted batch. This is plotted in Figure 3 over the temperature range of interest, from melting temperature $T_m(1123\,\text{K})$ to the gas temperature $T_g(1850\,\text{K})$. For later purposes note that the effective conductivity greatly exceeds the ordinary conductivity and that the rate of increase is almost linear over the temperature range of interest.

Both the above models assume the scattering surfaces (solid material, bubbles etc.) are uniform and uniformly distributed through the melt which is not true in the present case, but one would expect and we will show that the results obtained are reasonably insensitive to such details.

[1] i.e. zones in which the length scale associated with temperature variations is much larger than the mean distance of penetration of photons.

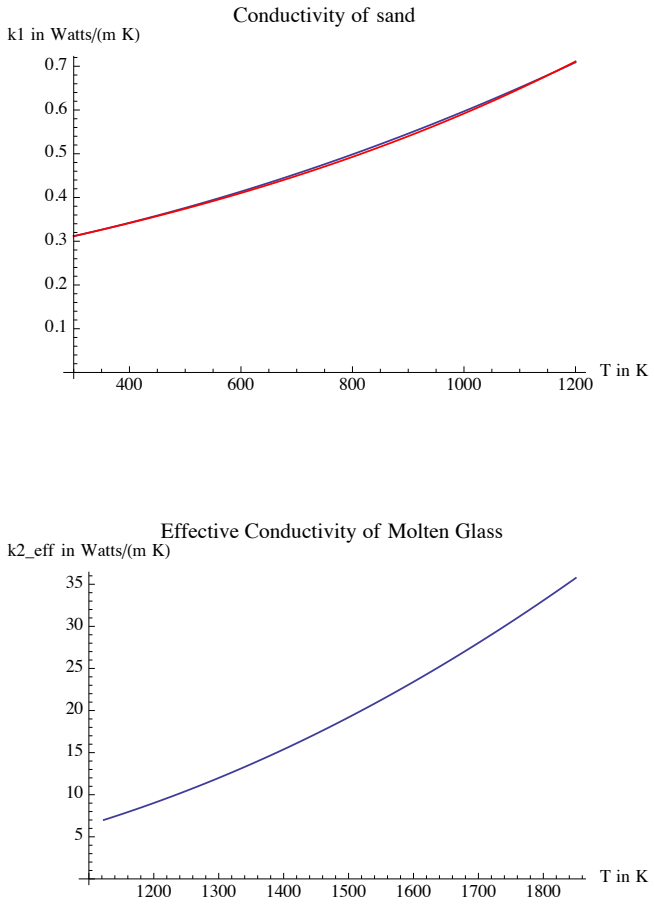

Figure 3: Batch conductivity: *Upper:* Conductivity $k_1(T_1)$ of sand. *Lower:* Effective conductivity $k_{2\text{eff}}(T_2)$ of molten glass (a Rosseland approximation).

2.2 Important parameter combinations

Firstly it is useful to estimate some of the key parameter combinations. We will use the following parameters taken primarily from Wu and Viskanta (1986) and Khun (2002).

Unreacted Batch Parameters

$c_1 = 1 - 1.1 \times 10^3$ Ws/kg K

$\rho_1 = 1.4 \times 10^3$ kg/m^3

$k_1 = 0.3116 \exp(0.275(T/300 - 1))$W/m K

$\epsilon_1 = 0.7$

$T_0 = 300$ K

Melt Parameters

$c_2 = 1.42 \times 10^3$ Ws/kg K

$\rho_2 = 1.4 - 2.32 \times 10^3$ kg/m^3

$k_{2\text{eff}} = 5.39 - 0.0217 \times T + 0.0000206 \times T^2$ W/m K

State Change Parameters

$\sigma = 5.7 \times 10^{-8}$ (Stefan-Boltzmann constant)

$T_m = 1123$ K

$T_R = 1800 - 2300$ K

$T_g = 1850$ K

$\Delta h_m = 5.65 - 7.5 \times 10^5$ Ws/kg (Kuhn 7.5)

$T_b = 1500$ K

$\mu = 50$ W/m^{2}K.

2.3 Observations and estimations

In order to determine the important features of the problem we will estimate the processes involved; later approximations will be based on these observations. The batch is fed into the furnace in loose piles which subsequently compact and settle out. In accordance with Wu and Viskanta (1986) we will assume a batch layer thickness varies from about 2 to 4 cms. Furnace simulations by Wu and Viskanta suggest overall melting time of a 2 cm depth batch to be about 130 secs and 350 secs for a 4 cm layer, which are consistent with observations.

2.3.1 The Stefan number

Of major importance for the melting process is the ratio of the heat required to raise the temperature of the batch from its initial value ($T_0 = 300\,\mathrm{K}$ (say)) to the melting temperature $T_m = 1123\,\mathrm{K}$, to the latent heat required to melt the batch, a ratio referred to as the Stefan number. Using the parameters above (and ignoring the heat required to dry the batch) we obtain

$$\mathcal{S} = \frac{\text{SensibleHeat/kg}}{\text{Reaction Heat/kg}} = \frac{c_1(T_m - T_0)}{\Delta h_m} \approx 1.6, \tag{5}$$

which indicates that the sensible and latent heat requirements for the melting process are of the same order. Evidently preheating the batch could significantly effect the melting time in the furnace, see later.

2.3.2 The time to reach melting point

Sand is a poor conductor so one would expect the time required to raise the surface of the batch to the melting point of the sand to be relatively small; we will estimate this time. The surface temperature rise of a semi-infinite body of conductivity k_1 due to a constant heat flux q into the surface from time $t = 0$ is given by

$$T_h = \frac{q}{\sqrt{\pi \rho_1 c_1 k_1}} \sqrt{t},$$

see Carslaw and Jaeger (1959). If in our case we take the heat input as being due (only) to flame radiation, then $q = \epsilon \sigma T_R^4$ and this gives a pre-melting time scale of 8.6 secs (if one uses $k_1 = 0.31\mathrm{W/m\ K}$) to 18.4 secs (if one uses $k_1 = 0.66\mathrm{W/m\ K}$). These values are very much less than the observed melting time of the batch in the furnace (typically 130 to 350 secs).

The bottom of the batch layer is in direct contact with the molten glass in the furnace at temperature $T_b \approx 1500\,\mathrm{K}$ so the melting will be immediately initiated on the underside of the batch.

2.3.3 Conduction time scales

In the absence of melting the time required for heat to conduct through an unmelted batch layer of thickness h is approximately

$$t_1 = h^2/\kappa_1, \text{ where } \kappa_1 = k_1/(\rho_1 c_1). \tag{6}$$

The conductivity of sand increases from 0.35 to 0.66 W/m K over the temperature range (room temperature to melting temperature), see Figure 3 Left, giving a conduction time of order $t_1 = 15.5 - 29$ mins for a 2 cm layer, and four times this for a 4 cm layer. As indicated earlier the entering batch consists of overlapping piles of different depth; 1 hour seems a sensible (under) estimate. This is much longer than the observed time for melting (130-350 secs), so conduction through sand is not the 'controlling factor' for the overall melting process.

In the absence of radiative input the conductivity of molten silica glass ranges from $0.6 - 1.2$ W/(mK), see Shibata et al (2005) and Schick et al (2012) with little variation with temperature. However, as indicated earlier, the effect of radiative exchanges within the melt is to increase the effective conductivity of molten glass by a factor of about 5 (35.7/7) over the temperature range $T_m = 1123$ K to $T_g = 1850$ K of interest, see Figure 3. Taking the higher temperature as being most appropriate for time estimates this gives a time scale of

$$t_2 = h^2/\kappa_2 \text{ where } \kappa_2 = k_{2\text{eff}}/(\rho_2 c_2); \tag{7}$$

which gives 36 secs for a 2 cms layer (43 secs if use Kuhn), and four times this for a 4 cm layer. This value is less than 1/3 of the observed furnace melting time and suggests that the molten batch behaves as a good conductor because of radiative exchanges.

2.3.4 Radiative input melting time

If radiation alone provided the latent heat to melt the batch then the time required would be

$$t_R = \frac{\rho_1 \Delta h_m h}{\epsilon \sigma (T_R^4 - T_m^4)}, \tag{8}$$

where we have taken into account re-radiation from the front at the melting temperature T_m. The range usually quoted for T_R is 1800 K to 2100 K, and the quoted Δh_m range is $5.6 - 7.5 \cdot 10^5$ Ws/kg, and if we take $\epsilon = 0.5$, we obtain a melting time of t_R of 30 secs to 50 secs for a 2 cm batch layer, and twice this for a 4 cm layer. There is considerable uncertainty about the net radiative input, but the time required is of the same order but somewhat less than the observed furnace melting time. Of course the radiative input needs to also supply sensible heat, so this underestimate is to be expected.

It can be seen from the above that the effect of multiple reflections within the melting batch is to greatly increase the conductivity (by a factor of about

30) of the melt and thus greatly reduce the expected melting time from about 1 hour down to about 2 minutes. One would expect the actual front speed $\dot{s}_1$ to be much greater than the solid batch conduction speed t_2 but somewhat greater than the radiative melting speed t_R.

2.3.5 Radiation versus convection

Both the radiative input from the flames and convection/conductive heat transfer from the gas in contact with the batch serve to melt the batch; the gas temperature T_g is larger than the melting temperature T_m. The ratio

$$\mathcal{K} = k_{2\text{eff}}(T_g - T_m)/\left[\epsilon\sigma(T_R^4 - T_m^4)h\right] \tag{9}$$

provides a useful comparison of these two inputs. For a 4 cm batch layer using upper and lower values for $k_{2\text{eff}}$ gives a $\mathcal{K}$ in the range $0.2 - 1.1$. It is clear from this that both processes play a role in the conversion.

The estimates above are in accord with observations, and suggest that the melting front speed is very much greater than the (solid) batch conduction 'speed' but somewhat less than the melt conduction 'speed'.

2.4 A simplified model

As indicated above the radiant heat is absorbed throughout the melt and $s(t)$ is identified as being the location where melting first occurs. There will be a zone above this location which consists of partially melted batch, however, as a simplification, we will assume that the absorption and melting all occur *at* the location given by $s(t)$, with melted glass above this location, and unconverted batch below. Under such circumstances the appropriate condition to impose at the front is the Stefan condition

$$\epsilon\sigma(T_R^4 - T_m^4) + q_{1s} - q_{2s} = -\rho_1 \Delta h_m \frac{ds}{dt}, \tag{10}$$

where Δh_m is the latent heat per unit mass to convert sand into molten glass, $q_{2s} = -k_{2\text{eff}}(T_m)\frac{\partial T_2}{\partial z}$ is the heat flux from the front into the molten batch, and $q_{1s} = -k_1(T_m)\frac{\partial T_1}{\partial z}$ is the heat flux from the unconverted batch into the front, see Figure 2 (both are negative). Also the front is at the melting temperature T_m which requires

$$T_1(z,t) = T_2(z,t) = T_m \text{ at } z = s(t). \tag{11}$$

With the Rosseland approximation in place, and local latent heat terms relegated to the melting front, the heat equation in the melt becomes

$$\rho_2 c_2 \left[\frac{\partial T_2}{\partial t} + (1 - \frac{\rho_1}{\rho_2}) \frac{ds}{dt} \frac{\partial T_2}{\partial z} \right] = \frac{\partial}{\partial z} \left(k_{2\text{eff}}(T) \frac{\partial T_2}{\partial z} \right) \text{ in } z > s(t). \tag{12}$$

The heat equation in the batch remains

$$\rho_1 c_1 \frac{\partial T_1}{\partial t} = \frac{\partial}{\partial z} \left(k_1(T) \frac{\partial T_1}{\partial z} \right), \quad z < s(t). \tag{13}$$

At the top surface we assume the heat exchange between the melt and the gas at temperature T_g to be adequately described by a Robin condition

$$q_{2h} = -k_{2\text{eff}}(T_h(t)) \frac{\partial T_2(h)}{\partial z} = \mu (T_h(t) - T_g), \tag{14}$$

where (ignoring the density changes) $T_h(t) = T_2(h,t)$ is identified as the surface temperature of the melt, q_{2h} the heat flux through the surface of the melt and where μ is the heat transfer coefficient. In practice the gas temperature T_g is determined by the geometry and global furnace heat conservation considerations, and may be modelled, however for present purposes we will assume that T_g is prescribed and can be adjusted by suitable modifications to the furnace, for example by altering the gap between the molten glass and the flame.

2.5 Analysis of the melt (Zone 2)

Based on our previous observations we anticipate a quasi-steady solution for the temperature within the melt with a slowly moving front. In this zone it is appropriate to use T_m as a datum and to use $(T_g - T_m)$ as the temperature scale; we use the scaling

$$z = hz', s = hs'(t'),\ t = t_R t',\ T_2 = T_m + \Delta T_2\ T_2',\ \Delta T_2 = (T_g - T_m), \tag{15}$$

$$q_{2h} = [\mu\ \Delta T_2]\, q'_{2h},\ \text{and } k_{2\text{eff}}(T_2) = k_{2m} k'_2(T'_2),\ \text{where } k_{2m} \equiv k_{2\text{eff}}(T_m) \tag{16}$$

is the effective conductivity of liquid glass at the melting point. Note that we have used the radiation time scale t_R identified earlier, see (8).

Assuming a quasi-steady profile and ignoring volumetric changes, the heat equation (12) reduces to its dimensionless form

$$-\frac{\partial}{\partial z'}\left[k_2'(T_2')\frac{\partial T_2'}{\partial z'}\right] = 0,$$

so integrating with respect to z' and applying the surface condition (14) we obtain (after scaling):

$$-k_2'(T_2')\frac{\partial T_2'}{\partial z'} = q_{2h}', \text{ with } q_{2h}' = q_{2s}' = (T_h' - 1).^2 \tag{17}$$

We have a fixed heat flux q_{2h}' through the zone determined by the heat transfer rate through the surface of the melt. The surface temperature T_{2h}' is not yet explicitly determined. Integrating again, and noting that $T_2' \to 0$ at the melting front $s'(t')$ we obtain

$$\int_0^{T_2'} k_2'(T_2')dT_2' = q_{2h}'(s'(t') - z') = (T_h' - 1)(s'(t') - z').$$

This equation implicitly determines the temperature field $T_2'(z)$ through the melt. We require $T_2'(1) = T_h'$, which gives the consistency result

$$\int_0^{T_h'} k_2'(T_2')dT_2' = (T_h' - 1)(s'(t') - 1), \tag{18}$$

which can be solved for T_h' for any prescribed $k_2'(T_2')$. The left hand side is the temperature averaged conductivity of the melt. As noted earlier, and see Figure 3, the variation of the conductivity over the (scaled) temperature range 0 to 1 is almost linear, so with little error we can write

$$k_2'(T_2') = 1 + T_2'(k_{2g}' - 1),$$

see (16), where $k_{2g}' = k_2'(1)$, is the (effective, scaled) conductivity of the melt at the gas temperature. This approximation greatly simplifies the analysis. The consistency result (18) then gives

$$T_h' + (k_{2g}' - 1)(T_h')^2/2 = (T_h' - 1)(s'(t') - 1),$$

[2]Note that $T_h = T_m + \Delta T_2 T_h'$.

which determines the surface temperature and associated heat flux as

$$T'_h = \frac{1}{(k'_{2g}-1)}\left[\sqrt{1+(1-s')\left[2k'_{2g}+(1-s')\right]}-(2-s')\right],\ q'_{2h}=(T'_h-1), \tag{19}$$

see (17). Figure 4 displays the scaled surface temperature T'_h as a function of the location of the front position s'; the data described earlier is used here. Note that the temperature of the surface is initially at the melting temperature corresponding to $s'=1$, and it gradually increases to reach values close to the scaled gas temperature $T'_2=1$ as melting proceeds and $s'\to 0$.

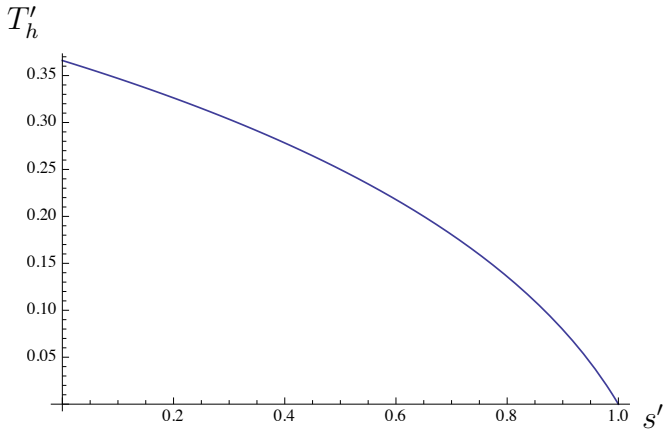

Figure 4: The scaled surface temperature of the melt as a function of the (scaled) location $s'(t)$. The gas temperature (1850 K in this case) is scaled to unity and the melt temperature (1123 K) is scaled to 0 and batch depth (4 cm) is scaled to unity.

In dimensional terms the conductive heat flux through the melted batch is given by

$$q_{2s}=q_{2h}=[\mu\Delta T_2]\,(T'_h-1); \tag{20}$$

again note that $q_{2h}<0$ so that heat from the combustion gases assists batch melting.

2.6 Batch analysis (Zone 1)

In this zone it is appropriate to use the room temperature T_0 as a datum and use $(T_m - T_0)$ to scale the temperature rise. Explicitly we use the scales

$$z = hz', s = hs'(t'),\ t = t_R t',\ T = T_0 + \Delta T_1\ T_1',\ \text{with } \Delta T_1 = (T_m - T_0), \quad (21)$$

$$\text{and } k_1(T_1) = [k_{10}]k_1',\ k_1' = e^{\gamma_0 T_1'},\ \text{with } \gamma_0 = \gamma(T_m/T_0 - 1), \quad (22)$$

$$\text{and } q_1 = \left[\frac{k_{10}\Delta T_1}{h}\right] q_1',\ \text{with } q_1' = -k_1'(T_1')\frac{\partial T_1'}{\partial z'}, \quad (23)$$

see (22), where k_{10} is the conductivity of the batch at room temperature T_0, and q_1' the scaled flux from the unconverted batch into the front, see Figure 2.

We anticipate a travelling wave solution of the scaled form

$$T_1' = T_1'(\zeta') \text{ where } \zeta' = s'(t') - z',\ \text{with } T_1'(0) = 1,\ \text{and } T_1'(\infty) = 0, \quad (24)$$

where the wave speed $\dot{s}'$ is assumed to be constant in accordance with our quasi-steady approximation and where we have anticipated that the thickness of the front is small compared with the thickness of the batch. Substituting into the heat equation (13) we obtain (after scaling)

$$\lambda \dot{s}_1' \frac{\partial T_1'}{\partial \zeta'} = \frac{\partial}{\partial \zeta'}\left(k_1'(T_1')\frac{\partial T_1'}{\partial \zeta'}\right),\ \text{where } \lambda = \frac{h^2\rho_1 c_1}{k_{10}t_R} \equiv \frac{t_c}{t_R} \gg 1\ , \quad (25)$$

see (6, 22). This integrates to give

$$\lambda \dot{s}_1' T_1' = k_1'(T_1')\frac{\partial T_1'}{\partial \zeta'}\ , \quad (26)$$

after requiring that $T_1' \to 0$ as $\zeta' \to \infty$, see (24). Evaluating this at the front $\zeta' = 0$ where $T_1' = 1$ gives

$$\lambda \dot{s}' = k_1 T_1'(0)\frac{\partial T_1'}{\partial \zeta'}(0) = -q_1'(0) \equiv -q_{1s}', \quad (27)$$

so the unscaled heat input from the front into the unconverted batch is given by

$$-q_{1s} = -\left[\frac{k_{10}\Delta T_1}{h}\right]\lambda \dot{s}' \equiv -\left[\frac{h\rho_1 c_1 \Delta T_1}{t_R}\right]\dot{s}', \quad (28)$$

using (25), which simply states that the sensible heat input ($-q_{1s}$) required to raise the temperature of sand to the melting temperature needs to be supplied by conduction from the front.

Equation (26) integrates to give

$$-\lambda \dot{s}_1' \zeta' = \mathrm{Ei}(\gamma_0 T_1') - \mathrm{Ei}(\gamma_0),$$

where Ei is the exponential integral function. For T_1' small we obtain $T_1' \approx e^{-\lambda \dot{s}_1' \zeta'}$, so heat from the travelling front penetrates a scaled distance of order $1/\lambda \ll 1$ into the unreacted batch. In dimensional terms this gives a distance of order $k_1^0/(\rho_1 c_1 \dot{s})$. Using the values presented earlier we obtain a penetration distance of 1 mm and 2 mm for batch depths of 2 cm and 4 cm respectively; as anticipated the penetration distance is relatively small compared with the batch thickness.

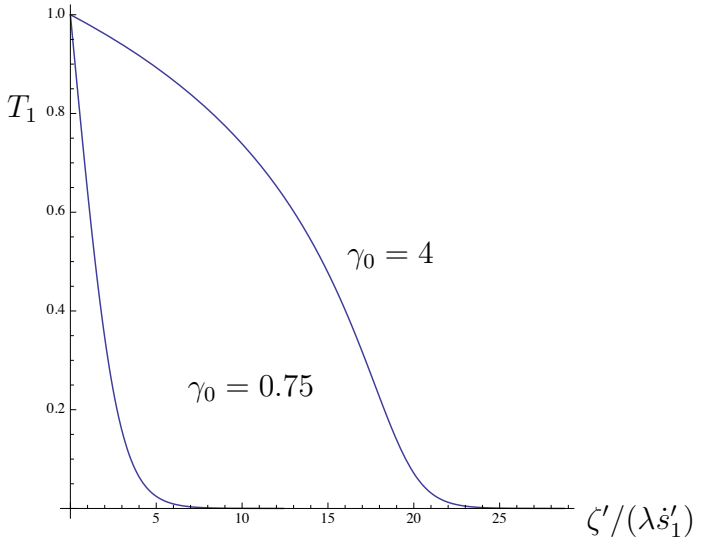

Figure 5: The scaled temperature variation $T_1(\zeta')$ through the upper melting front for $\gamma_0 = 0.75$ and $\gamma_0 = 4$.

The temperature variation through the melting front is displayed in Figure 5. The profile shape is strongly dependent on the value of γ_0, see (22), which provides a measure for the effect of the input temperature of the batch T_0 on the front structure. The listed values for T_0 and T_m give $\gamma_0 = 0.75$ and for comparison the results for $\gamma_0 = 4$ are also presented. Note that the

front is significantly flatter and thicker if T_0 is smaller; preheating can strongly affect the heating history of a batch particle.

2.7 The Stefan condition

The various components of heat transfer into and out of the front have now been determined and when substituted into the Stefan condition (5) give

$$[\mu\Delta T_2]\,(T_h'-1) - \left[\frac{h\rho_1 c_1 \Delta T_1}{t_R}\right]\dot{s}' = \left[\epsilon\sigma(T_R^4 - T_m^4)\right] + \left[\frac{\rho_1 \Delta h_m h}{t_R}\right]\dot{s}', \qquad (29)$$

see (20, 28). That is

$$\dot{s}'\left(\left[\frac{h\rho_1 c_1 \Delta T_1}{t_R}\right] + \left[\frac{\rho_1 \Delta h_m h}{t_R}\right]\right) = -\left[\epsilon\sigma(T_R^4 - T_m^4)\right] + [\mu\Delta T_2]\,(T_h'-1).$$

Rearranging and recalling that the time scale t_R was chosen so that the net radiative input and latent heat requirements are in balance, we obtain

$$\dot{s}'\,(1+\mathcal{S}) = -1 + \mathcal{K}(T_h'(s')-1); \qquad (30)$$

an ordinary differential equation determining the movement of the front. The important dimensionless groups are the already identified Stefan number $\mathcal{S}$ (see (5)) and the convective heat transfer parameter $\mathcal{K}$ (see (9)), which determines the relative proportion of heat input into the front from the combustion gas compared to direct radiative input. As seen earlier the Stefan number is approximately 1.6 for the prescribed conditions. Evidently it is appropriate to rescale time using the 'melting' time scale

$$t_m = t_R(1+\mathcal{S}), \text{ and with } t'' = t_m t', \qquad (31)$$

see (8, 5), which takes into account that both sensible and latent heat need to be supplied to the batch for conversion. The melting time is thus about $(1+1.6)t_R \approx 130-260$secs for 2cms and 4cms respectively. This matches up with the numerical simulations of Wu and Viskanta (1986). The rescaling gives

$$\frac{ds'}{dt''} = -1 + \mathcal{K}(T_h'(s')-1),$$

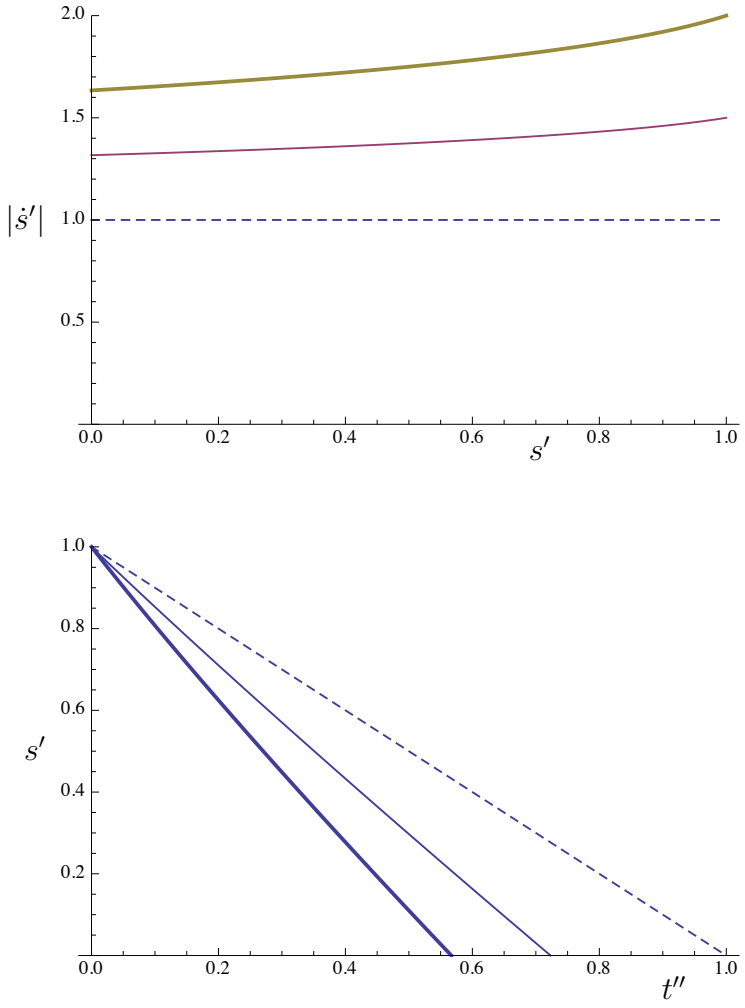

Figure 6: Scaled front speed for $\mathcal{K} = 0, 0.5, 1.0$ (dashed, thin, thick): $|\dot{s}'(t'')|$; *Upper*: The front speed $\frac{ds'}{dt''}(s')$ as a function of location. *Lower*: The front location as a function of scaled time, $s'(t'')$, as in (31).

an exactly solvable separable ODE for $s'(t'')$. Previous estimates give a $\mathcal{K}$ range going from 0.12 to about 1.1, depending on the combustion gas and effective radiation temperatures. A plot of $\dot{s}'(s')$ and $s'(t'')$ for a range of values of $\mathcal{K}$ is shown in Figure 6. In the $\mathcal{K} = 0$ case (the dashed curves), there is no heat transfer from the combustion gases, and in this case the front travels with constant speed and the melting time is $t_m = t_R$. Increasing values of $\mathcal{K}$ correspond to increasing additional convective transfer from the combustion gases (thin and thick curves) the melting rate increases by up to a factor of about 2. The implication is that reducing the depth of the furnace can significantly influence the melting time.

Note that the front speed marginally decreases as melting proceeds due to the changed effective conductivity of the melt. A useful approximation can be obtained by simply averaging the right hand side of (30) to give the constant front speed of

$$|\dot{s}'| = \frac{1 + \mathcal{K}\mathcal{F}(k'_{2g})}{(1 + \mathcal{S})} \tag{32}$$

where

$$\mathcal{F}(k'_{2g}) = 1 + \frac{1}{2(k'_{2g} - 1)} \left(\sqrt{2 + 2k'_{2g}} + \sqrt{1 + 2k'_{2g}} - 3 \right) .$$

Interpreting this one can see that the effect of combustion gas on front speed is to increase it by the factor $(1 + \mathcal{K})\mathcal{F}(k'_{2g})$ which primarily depends on the abrupt change in conductivity across the front but also depends on the relative change in effective conductivity across the melt.

2.8 The lower melting front

The lower melting surface of the batch is in contact with melted glass at a temperature greater than the melting point with the cooled glass being refreshed continuously. The temperature variations under the batch as it moves into the furnace are relatively small (250 K verses $T_{melt} \approx 1200$ K) so that the heat transfer driving the lower front will remain almost constant and the front speed will remain at a constant value given by

$$\dot{s_b} = \mu_1 \frac{(T_b - T_m)}{\rho_2 \Delta h_m},$$

where μ_1 is the heat transfer coefficient. This front speed is relatively small compared with the radiation driven upper front $\dot{s}$ and would be best measured

or inferred from observations. The temperature profile near this front is the same as that obtained for the upper front; importantly the thickness of the front is small and so the two fronts act independently until they begin to overlap.

2.9 Summary and conclusions

The quantitative results obtained in this work mirror the simulations already obtained by Wu and Viscanta (1986) but the results here are analytic and as such provide a better understanding of the processes involved. The front speed has been found to be inversely proportional to the Stefan number and directly proportional to $\mathcal{K}'$ so that for example the effect of preheating (or the effect of moisture in the batch) is simply to reduce the melting time in the obvious way. The effect of increasing the combustion gas temperature, by for example reducing the spacing between the flames and the batch, is again simply described. The temperature profile is linear within the melt with a boundary layer transition through the unmelted batch.

The above results may be used to determine the thermal history of batch particles and thus the propensity of the batch to shed bubbles of various sizes into the bath. Also global heat transfer estimates within the furnace can be made based on the above results and may be used to assist with the design of the furnace.

3 Development and movement of bubbles in the furnace

There was insufficient time at the MISG to work on this problem but the summary below and some preliminary ideas concerning model development may provide a useful starting point for further work.

3.1 Flow in the furnace

Cold floating materials are added at one end of the furnace which is heated by flames from above. The effect of the floating batch is to partially shield the molten glass in the bath from incoming radiation so that a hot spot is produced just ahead of the batch and two convection cells are generated; a primary cell with glass sinking down the entry wall and a secondary cell with

glass sinking down the exit wall, see Figure 1. The size and strength of these two cells is effected by the length of the floating batch, the nonuniform flame heating from above, entry and exit flow conditions, and the presence of barriers and bubblers inserted into the top and bottom of the chamber. The two cells play different roles. The primary cell homogenises and purifies the batch by removing defects (bubbles, seeds and unresolved material). Fining agents (antimony and arsenic oxides) added to the batch assist in the bubble removal process by releasing large amounts of gases (nitrogen oxide and oxygen) that sweep up small bubbles while travelling to the surface; higher temperatures are required for this fining process within the primary cell. The secondary cell is at a lower temperature. The objective here is to shrink the remaining bubbles with the gas being absorbed.

Melted batch particles sink into the bath and are carried backwards in the primary convection cell towards the batch entry point and then forwards towards the hot spot where they rise towards the surface and either remain within the primary cell (and thus are returned to the chamber entry point) mixing with newly melted batch along the way or are caught up in the secondary loop where they circulate until they exit the chamber. The residence time of particles is typically 10-15 hours but can be as long as 60 hours. Evidently this uncertainty in the residence time is problematic.

3.1.1 Flow details

The effect of the thermal gradient along the upper surface of the molten glass is to cause a buoyancy driven circulatory flow with volume and heat flux (per unit depth of the 2D furnace) levels of order $\kappa(A/L)$ and $\rho c\Delta T(\kappa(A/L))$, where ΔT is the typical temperature difference over the length L of the furnace and A the depth of the furnace. The strength of the flow is determined primarily by the Rayleigh number defined by

$$Ra = \frac{g\alpha\Delta T L^3}{\nu\kappa},$$

where κ is the thermal diffusivity, ν the viscosity and α the thermal expansivity. In the glass furnace context Ra is large (of order $10^4 - 10^6$) and under such circumstances most of the flow occurs in thin boundary layers of thickness $Ra^{-1/5}L$, with compensationally higher velocities $\kappa/LRa^{1/5}$, with the flow sinking (downwelling) at the cold left end of the furnace and rising at the hot end with an associated surface flow from hot to cold. Typical melt velocities

are 10^{-3} m/sec, see Howell and Ockendon (2007). It is not clear if the returning flow occurs immediately below the surface flow (intrusive flow above a strongly stratified flow) or occurs at the bottom of the furnace, see Chui-Webster, Hinch and Lister (2008) and Gramberg, Howell and Ockendon (2007). Experiments suggest that under linear gradient conditions intrusive flow is more likely, however, in the glass furnace case inertia and shear instabilities are likely to be generated and one would expect the return flow to occur throughout the lower region. The actual heating arrangements are very different from the theoretically investigated situations described above with two cells being deliberately forced by the firing arrangements, the presence of a barrier and the introduction of bubbles. Simple modelling (experimental and mathematical) followed up by numerical simulations may provide useful information about the effectiveness of these cell generation mechanisms.

As indicated earlier the residence time for batch particles varies significantly because particles rising near the hot spot can remain within the primary loop or be caught up in the secondary loop and the presence of transients and eddies in the flow will strongly effect the outcome; such flow variability issues are likely to be harder to address.

3.2 The bubbles

A good description of the formation and growth of gas bubbles within a super saturated liquid and the behaviour of foams formed on the surface can be found in Weaire and Hutzler (1999). Also, in context the authors found the MISG report by Power et al (2010) on 'The Initiation of Guinness' to be particularly informative and relevant. We briefly summarise the background required in the present context.

Gas molecules diffuse across any liquid to the gas interface. Under saturated conditions a balance is realised between the flux of gas molecules into and out of the interface, a result that is quantified in Henry's Law

$$c_l = H(T)p,$$

where c_l is concentration of the gas in the liquid, p is the partial pressure of the gas of interest and H is Henry's law 'constant' which decreases as the temperature T increases. This result applies across flat interfaces and adjustments are required for curved surfaces.

In the bubble situation (and with a single gas), the gas pressure p_b inside a bubble of radius R exceeds that in the liquid immediately outside p_l according

to Laplace's law

$$p_b = p_l + \frac{2\gamma}{R},$$

where γ is surface tension of the liquid in contact with the gas. The effect of mass transfer across the surface of the bubble will be to increase or decrease its size until equilibrium is reached with the concentrations of the gas inside and outside in balance. This will occur when $c_l = Hp_b \equiv c_b$ and $R = R_{\text{crit}}$ where

$$c_l = H(p_l + \frac{2\gamma}{R_{\text{crit}}}) \text{ so } R_{\text{crit}} = \frac{2\gamma}{c_l/H(T) - p_l}; \tag{33}$$

there is an equilibrium bubble (critical) radius R_{crit} determined by (local) pressure, temperature and concentration levels within the liquid. This equilibrium state is however unstable and so cannot be realised. If $R < R_{\text{crit}}$ then $c_b > c_l$ and molecules diffuse out of the bubble and it shrinks further. If $R > R_{\text{crit}}$ then $c_l > c_b$ and the bubble further expands. The implications are that bubbles of size $R < R_{\text{crit}}$ immediately collapse, and so cannot be formed within the (constant c_l) region in the first place, and bubbles of size $R > R_{\text{crit}}$ continue to grow. In our glass furnace case gas is emitted as a result of the chemistry so that bubbles with size $R > R_{\text{crit}}$ will be formed within the melt itself. The role of fining materials is to supply such bubbles. Also bubbles will be brought into the melt from the batch. The presence of nucleation sites within the melt can strongly influence the number of bubbles.

A primary aim of the furnace operation is the remove gases either brought into the melt with the batch or produced by the melting process, so a significant proportion of these gases must be removed by the bubbles. Under such circumstances one would hope for or anticipate the presence of many bubbles and expect (really require) significant changes in concentration of gases in the melt. If bubbles are produced in sufficient numbers then the gas concentration in the melt will reduce and an equilibrium situation can arise in which the bubble size asymptotically approaches an equilibrium value consistent with the concentration of gas within the liquid; explicitly the bubbles will continue to grow until the dissolved gas concentration reduces to

$$c_l = H(p_l + \ 2\gamma/R_\infty),$$

where R_∞ is the asymptotic equilibrium radius, as required by Henry's law. Knowing the initial concentration of gas in the melt one can estimate (c_l, R_∞).

3.3 Bubble residence time

Buoyancy forces acting on bubbles either carried into, or formed within, the molten glass bath will cause the bubbles to rise out of the bath and burst on the surface, and the primary issue here is to determine how the residence time of such bubbles depends on the operating conditions within the furnace. Complications arise because the bubbles are formed in different locations and are initially small and so will be carried by the convection flow to different locations with different temperature, pressure and gas concentration conditions. Under such circumstances a simple crude model is indicated. The analysis undertaken in the guinness context will be modified to deal with the present context.

The bubble has a radius $R(t) > R_{\rm crit}(c_l)$ in its initial location with gas concentration in the melted glass given by c_l and so will initially grow due to the transfer of gas from the surrounding melt. The rate of growth of the bubble is described by

$$\frac{d}{dt}(\frac{4}{3}\pi R^3\rho_b) = k4\pi R^2\Delta c \tag{34}$$

where ρ_b is the density of gas within in the bubble, $\Delta c = (c_b - c_l)$ is the difference in gas concentration between gas within the bubble $c_b(t)$ and the liquid outside the bubble c_l, and k is the mass transfer coefficient. Assuming the gas within the bubble obeys the perfect gas law its density will be determined by its temperature T_b

$$\rho_b = p_b/(\mathcal{R}T_b); \tag{35}$$

$\mathcal{R}$ the gas constant and T_b the absolute temperature of the bubble gas. Note that the temperature of gas within the bubble will be the same as that of the neighbouring molten glass and the relative variation of the T_l will be small within the bath, as will be the pressure variations (as far as the gas is concerned). The pressure within the bubble will exceed that within the liquid due to surface tension according to Laplace's law

$$p_b = p_l + \frac{2\gamma}{R(t)}, \tag{36}$$

where γ is the surface tension which one would not expect to vary significantly over the temperature range within the bath. The gas density in the bubble will thus vary according to the result

$$\rho_b = \rho_0(1 + \frac{\epsilon}{R(t)}), \text{ where } \rho_0 = \frac{p_l}{\mathcal{R}T_b} \text{ and } \epsilon = \frac{2\gamma}{p_l};$$

ρ_0 is the density of the gas under atmospheric pressure at the temperature of the bath (1500 K), using (36, 35). The gas density will thus be almost constant for $R > \epsilon$.

Using the above results we can determine the change in radius of the bubble brought about by transfer across its surface as:

$$\frac{dR}{dt}\left[1 + \frac{2}{3}(\frac{\epsilon}{R})\right] = \frac{k}{\rho_0}\Delta c. \tag{37}$$

Note that the radius changes linearly with time in a constant concentration environment for $R \gg \epsilon$. However also note that the initial growth rate is small for small radius bubbles due to the excess pressure within the bubble. The time scale for growth due to mass transfer across the bubble surface is $t_b = \frac{\rho_l R_0}{k\Delta c_0}$ for $R_0 \gg \epsilon$ but increases to $t_b(R_0/\epsilon)$ for small radius bubbles.

The bubble will rise due to buoyancy and this tendency to rise will be opposed by viscous forces. The bubbles of interest are small and move slowly so the Reynolds number of the flow will be small and Stokes results are appropriate, see Batchelor (1967). The total drag D on a solid sphere of radius a moving with speed U through a liquid of viscosity μ is $6\pi a\mu U$, whereas that of a bubble is $4\pi aU$ due to induced flow within the bubble. In practice due to the effect of surface-active impurities the drag tends to be closer to that of a solid sphere at least in the water bubble context. In the gas bubble/molten glass context we will use

$$D = \alpha\pi R\mu U \text{ with } 4 < \alpha < 6,$$

to model in such effects; α would need to be determined experimentally. For vertical motion the terminal velocity is achieved if we have a balance between the buoyancy and the drag which gives a terminal velocity of

$$U = \frac{4}{3\alpha}\frac{R^2 g}{\nu_g}, \text{ where } \nu = \frac{\eta}{\rho_g} \tag{38}$$

and where ν is the kinematic viscosity of molten glass. In the temperature range from melting to 1550°C the dynamic viscosity varies by three orders of magnitude ($1 - 750$ Pa sec) and is adequately described by an Arrhenius model $\eta = A\exp(B/T)$ where A and B depend on composition, see Le Bourhis (2006) and Hrma (2006). The furnace operates at the higher end of the temperature rage so we'll use $\eta = 1$ Pa sec. The bubbles of interest range in radius from 3 mm down to 0.03 mm giving typical buoyancy speeds ranging from 4.5 cm/sec

down to 4.5×10^{-4} cm/sec for the smaller bubbles. Note that typical melt flow speeds are about 3×10^{-2} cm/sec which is comparable with the buoyancy speed for 0.2 mm radius bubbles. In crude terms bubbles larger than this will detach from the melt flow and reach the surface (say 1 m depth) in less than 1 hour and so are not of concern, and bubbles smaller than this radius will be carried along with the flow and have a strong probability of reaching the secondary cell.

We now outline the derivation of (38). The bubble (with effective zero mass) moving with velocity $\dot{\mathbf{r}}$ is imbedded in a prescribed flow field $\mathbf{V}(\mathbf{r})$ so that under quasi-steady conditions we have

$$(\mathbf{V} - \dot{\mathbf{r}})\alpha\pi R\mu + \rho_2(\frac{4}{3}\pi R^3)g\mathbf{k} = \mathbf{0}$$

and therefore

$$(\dot{\mathbf{r}} - \mathbf{V}) = \frac{4}{3\alpha}\frac{R^2 g}{\nu_g}\mathbf{k}. \tag{39}$$

Equations (37, 39) determine the motion and radius $R(t)$ of an individual bubble, however the concentration of gas in the molten glass surrounding the bubble will vary as the bubble moves through the melt so that a complete description of the flow environment would be required.

Without detailed flow simulations the best one can do here is to examine typical situations. Probably, however, such detailed investigations are of marginal interest.

Of more interest perhaps is a 'black box model' of the bubble production, growth, shrinkage and transfer process. We can consider the melt region as two regions (representing the two cells) separated by a barrier (representing the interface between the two cells). We can then assume an average temperature of T_1 for the first box , gas concentration in the liquid and a bubble size distribution under steady state conditions in the first box and use the above physics to determine the bubble size distribution in the second box given transfer rates across the barrier. When tied to experimental information this may lead to a workable model.

3.4 Observations/speculations/suggestions

It is evident that by tuning the present apparatus one might minimise bubble problems but the difficulty is one that is inherent to the apparatus; the variability of the batch element residence times.

It may be useful to note that rectified diffusion is successfully used to grow bubbles in guinness and may be applicable in the glass furnace situation. In the presence of a pulsating sound field a bubble of radius $R < R_{crit}$ will pulsate and there will be a net diffusion of gas into the bubble over a cycle so that it will grow providing the amplitude is greater than some threshold value. The effect is greatest if the resonance frequency of bubbles of interest is used.

4 Conclusions

The aim of this work has been to understand difficulties associated with the production of glass in the furnace. These difficulties are of an operational type (how to compensate for unexpected variations in batch input or processing) or of a quality type (as displayed in the flaw frequency). The primary focus in this report has been on operational issues. The available heat is used to melt and chemically convert the batch and the analysis suggests a constant front speed dependent on radiant heat input and the convective heat input through the upper surface. These results enable one to better estimate the heat requirements so that the overall heat balance can be better assessed and furnace design can be optimised. It is also hoped that a better estimate of the temperature development through the melt may be useful for understanding the chemistry.

References

1. Auchet, O. Riedinger, P., Malasse, O. and Iung, C (2008). First-principles simplified modelling of glass furnaces combustion chambers. *Control Engineering Practice* **16**, 1443-1456.

2. Batchelor, G. K., (1967) An Introduction to Fluid Dynamics. Cambridge University Press, Cambridge.

3. Carslaw, H. S. and Jaeger, J. C., (1959). Conduction of Heat in Solids., Clarendon Press, Oxford, p75.

4. Chiu-Webster S., (2007), Horizontal Convection and Glass Furnaces, and a Fluid Mechanical Sewing Machine; Cambridge University dissertation submitted to Trinity College.

5. Chiu-Webster S. Hinch, E. J. and Lister, J. R., (2008), Very viscous horizontal convection. *J. Fluid Mech.* **611**, 395-426.

6. Gramberg, H. J. J., Howell, P. D. and Ockendon, J. R., (2007). Convection by a horizontal thermal gradient. *J. Fluid Mech.* **586**, 41-75.

7. Howell, P. D., (1994). Extensional Thin Layer Flows, Ph.D. Thesis, St Catherines College, Oxford.

8. Hrma, P., (2006). High temperature viscosity of commercial glasses. *Ceramics*, **50**, 57-66.

9. Kuhn, W. S., (2002). Mathematical modelling of batch melting in glass tanks. In: Mathematical Simulation in Glass Technology, ed. Krause, D. and Loch, H., Springer, pp73-125.

10. Le Bourhis, E., (2006) Glass: Mechanics and Technology, Wiley.

11. Power, O. A., Lee, W., Fowler, A. C., Dellar, P. J., Schwartz, L.W. Lukaschuk, S. Lessells, G., Hegarty, A. F., O'Sullivan, M. Liu, Y., (2010). The initiation of Guinness, www.maths-in-industry.org food and drink report.

12. Rosseland, S., (1936) Theoretical Astrophysics, Clarenden Presss, Oxford.

13. Schick, V., Remy, B., Degiovanni, A. and Demeurie, F., (2012). Measurement of thermal conductivity of liquids at high temperature. *Journal of Physics, Conference Series* **395**, 1-8.

14. Shibata, H., Suzuki, A., and Ohta, H., (2005). Measurement of thermal transport properties for molten silicate glasses at high temperatures by means of a novel laser flash technique. *Materials Transactions*, **46**, 1877-1881.

15. Siegel, R and Howell, J. R. (2001). Thermal Radiation Heat Transfer, 4th edn. Taylor and Francis, Hemisphere.

16. Tooley, F. V., (1961). The handbook of glass manufacture. Ashlee Publishing Co. Inc. .

17. Weaire, D. and Hutzler, S., (1999). The Physics of Foams, Clarenden Press, Oxford.

18. Wu X. and Viskanta, R.,(1986). Modelling of heat transfer in the melting of a glass batch. *Journal of Non-Crystaline Solids*, **80**, 613-622.